Korean J. Chem. Eng., **28**(2), 567-574 (2011)
DOI: 10.1007/s11814-010-0388-z

Chemical absorption of carbon dioxide into oxirane solution containing ID-CP-MS41 catalyst

Kwang-Joong Oh*, Seong-Man Mun*, Seong-Soo Kim*, and Sang-Wook Park**,†**

*School of Civil and Environmental Engineering, Pusan National University, Busan 609-735, Korea
**School of Chemical and Biomolecular Engineering, Pusan National University, Busan 609-735, Korea
***Department of Environmental Administration, Catholic University of Pusan, Busan 609-757, Korea
(*Received 10 March 2010 • accepted 24 July 2010*)

Abstract−CP-MS41 was synthesized by hydrolysis of tetraorthosilicate, as a silicon source, with 3-chloropropyltriethoxysilane as an organosilane using cetyltrimethylammonium bromide as a template. ID-CP-MS41 was synthesized by immobilization of imidazole on the CP-MS41 and was dispersed in organic liquid as a mesoporous catalyst for the reaction between carbon dioxide and oxirane. Phenyl glycidyl ether and glycidyl methacrylate were used as oxiranes. Carbon dioxide was absorbed into the oxirane solution in a stirred batch tank with a planar gas-liquid interface within a range of 0-2.0 kmol/m^3 of oxirane and 333-363 K at 101.3 kPa. The measured values of absorption rate were analyzed to obtain the reaction kinetics using the mass transfer mechanism associated with the chemical reactions based on the film theory. The overall reaction of CO_2 with oxirane, which is assumed to consist of two steps--i) a reversible reaction between oxirane (B) and catalyst of ID-CP-MS41 (QX) to form an intermediate complex (C_1), and ii) irreversible reaction between C_1 and CO_2 to form QX and five-membered cyclic carbonate (C)--was used to obtain the reaction kinetics through the pseudo-first-order reaction model. Polar solvents such as *N*, *N*-dimethylacetamide, *N*-methyl-2-pyrrolidinone, and dimethyl sulfoxide affected the reaction rate constants.

Key words: Absorption, Carbon Dioxide, Oxirane, Imidazole, MCM-41

INTRODUCTION

The chemical fixation of carbon dioxide has become an important research topic because of the danger posed by global warming, and conversion of carbon dioxide into valuable substances is an extremely attractive solution. The reaction of CO_2 with oxiranes leading to 5-membered cyclic carbonates is well known [1], and these product carbonates can be used as polar aprotic solvents, electrolytes for batteries, and sources of reactive polymers [2]. The synthesis of cyclic carbonates by the reaction of CO_2 with oxirane has been performed using Lewis acids, transition metal complexes, and organometallic compounds as catalysts at high pressures, 10-50 atmospheres [3,4]. Milder conditions, however, atmospheric pressure in the presence of metal halides or quaternary onium salts, have been reported [5-10].

Research on oxirane-CO_2 reactions has focused on the reaction mechanism, the overall reaction kinetics, and the effect of the catalyst on the conversion [3-9]. Diffusion may affect the reaction kinetics in the mass transfer associated with the chemical reactions [11], so this effect is important to investigate the reaction kinetics of the gas-liquid heterogeneous reaction between CO_2 and oxirane. The kinetics of the reaction between CO_2 and oxiranes, such as phenyl glycidyl ether (PGE) and glycidyl methacrylate, have been studied using catalysts such as quaternary onium salts [12-15], polymer-supported catalyst with trialkylamine [16,17], and ionic liquid-supported catalyst with trialkylamine [18], The reaction rate constants were obtained using the measured absorption rate of CO_2, analyzed with the mass transfer mechanism associated with the chemical reactions.

Various functionalized catalysts such as polymers, amorphous, and fumed silica have mild activity due to the low accessibility caused by the low/non porosity. However, the discovery of the M41S family [19] generated a great deal of interest in the synthesis of organically functionalized, mesoporous materials for application in the fields of catalysis, sensing, and adsorption, based on their high surface areas and large ordered pores ranging from 20 to 100 Å [20] with narrow size distributions. Their high chemical and thermal stabilities are also promising for the reactions of bulky substrate molecules. In general, hybrid organic-inorganic materials have been prepared *via* post-grafting or co-condensation techniques. In 2000, a grafting technique was developed through a co-condensation method for hybrid MCM-41 using halogenated organosilanes [21]. Recently, a new synthetic approach has been developed for the preparation of hybrid inorganic-organic mesoporous materials based on the co-condensation of siloxane and organosiloxane precursors in the presence of different templating surfactant solutions [22]. Also, a new grafting technique was described for the synthesis of hybrid MCM-41 and trialkylamine-immobilized ionic liquids containing high catalytic activity for the synthesis of cyclic carbonates [23].

In this study, PGE or GMA and the mesoporous particle, ID-CP-MS41 [16], of imidazole-immobilized ionic liquid on hybrid MCM-41 were used as the reactant and catalyst in the reaction between CO_2 and oxirane, respectively, to investigate the absorption kinetics of CO_2 with a diffusion model, which is one of the series of works to investigate the capture and utilization of carbon dioxide.

†To whom correspondence should be addressed.
E-mail: swpark@pusan.ac.kr

THEORY

To determine the reaction kinetics between an oxirane and carbon dioxide using ID-CP-MS41 (QX) containing ionic liquid of imidazole, it is necessary to understand the reaction mechanism in a heterogeneous reaction. Although the reaction mechanism shown in Eq. (i) is assumed for homogeneous [3,6-9] and heterogeneous [17] oxirane-CO_2 reactions, no reliable evidence has yet been reported. The rate-determining step is the attack of the anionic portion of the catalyst on the oxirane. The importance of this portion of the catalyst can be explained by this mechanism, whereby the overall reaction between CO_2 and oxirane to form the 5-membered cyclic carbonate is as follows:

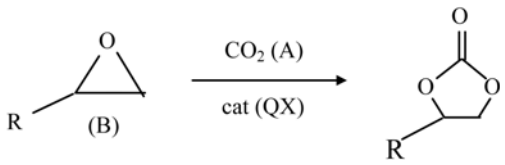

(i)

where R is a functional group of $-CH_2-O-C_6H_5$ of PGE, or $-CH_2-O-C(=O)-C(CH_3)=CH_2$ of GMA, respectively. The overall reaction of (i) in this study is assumed to consist of two steps: i) a reversible reaction between oxirane (B) and ID-MS41 (QX) to form an intermediate complex (C_1) and ii) irreversible reaction between C_1 and carbon dioxide (A) to form QX and the five-membered cyclic carbonate (C):

$$B + QX \overset{k_1}{\underset{k_2}{\leftrightarrow}} C_1 \quad \text{(ii)}$$

$$A + C_1 \xrightarrow{k_3} C + QX \quad \text{(iii)}$$

The reaction rate of CO_2 under the condition of a steady-state approximation to form C_1 is presented as follows:

$$r_A = \frac{C_B S_t}{\frac{1}{k_1} + \frac{1}{K_1 k_3 C_A} + \frac{C_B}{k_3 C_A}} \quad (1)$$

If the value of k_1 is very large, such that $1/k_1$ approaches 0, Eq. (1) is arranged to

$$r_A = \frac{C_A C_B S_t}{\frac{1}{K_1 k_3} + \frac{C_B}{k_3}} \quad (2)$$

Under the assumptions that B is a nonvolatile solute, the gas phase resistance to absorption is negligible by using pure CO_2, and thus Raoults' law applied. The mass balances of species A and B, using film theory accompanied by chemical reactions, and boundary conditions are given as follows:

$$D_A \frac{d^2 C_A}{dz^2} = r_A \quad (3)$$

$$D_B \frac{d^2 C_B}{dz^2} = r_A \quad (4)$$

$$z = 0;\ C_A = C_{Ai};\ \frac{dC_B}{dz} = 0 \quad (5)$$

$$z = z_L;\ C_A = C_{AL};\ C_B = C_{B0} \quad (6)$$

If the diffusion rate of CO_2 is not smaller than the reaction rate, and the amount of dissolved CO_2 that reacts in the diffusion film adjacent to the phase boundary is negligible, compared to the CO_2 which reaches the bulk liquid phase in the unreacted state, the concentration of A in the bulk liquid phase is a finite quantity (C_{AL}) and can be obtained from the following equation [11]:

$$k_L a_v (C_{Ai} - C_{AL}) = \frac{C_{AL} C_{Bo} S_t}{\frac{1}{K_1 k_3} + \frac{C_{Bo}}{k_3}} \quad (7)$$

In the general case that the reaction rate is given by Eq. (2), the material balance equations of component A and B based on the film theory, and the boundary conditions are put into the dimensionless form as follows:

$$\frac{d^2 a}{dx^2} = \frac{Mab}{1 + \alpha b} \quad (8)$$

$$\frac{d^2 b}{dx^2} = \frac{rqMab^2}{1 + \alpha b} \quad (9)$$

$$x = 0,\ a = 1,\ \frac{db}{dx} = 0 \quad (10)$$

$$x = 1,\ a = a_L,\ b = 1 \quad (11)$$

where $a = C_A/C_{Ai}$, $b = C_B/C_{Bo}$, $x = z/z_L$, $r = D_A/D_B$, $q = C_{Ai}/C_{Bo}$, $K_1 = k_1/k_2$, $\alpha = K_1 C_{Bo}$, $M = \alpha k_3 D_A S_t / k_L^2$, $k_L = D_A/z_L$.

The enhancement factor of CO_2 (β), defined as the ratio of the flux of CO_2 with chemical reaction to that without chemical reaction, is resented as follows:

$$\beta = -\left.\frac{da}{dx}\right|_{x=0} \quad (12)$$

At an initial absorption of CO_2, stating that C_B in the liquid film is constant as C_{Bo}, the reaction rate constants, K_1 and k_3, are obtained as follows;

Eq. (2) for the reaction between A and B is arranged as

$$r_A = k_o C_A \quad (13)$$

where k_o is the pseudo-first-order reaction rate constant.

The mass balance of species A with the film theory accompanied by a pseudo-first-order reaction is given as follows:

$$D_A \frac{d^2 C_A}{dz^2} = k_o C_A \quad (14)$$

From the exact solution of Eq. (14), β can be derived as follows:

$$\beta = \left.\frac{da}{dx}\right|_{x=0} = \frac{Ha}{\tanh Ha} \quad (15)$$

where Ha is the Hatta number, $\sqrt{k_o D_A}/k_L$.

The following equation, derived from Eq. (2) and (13), is used to obtain k_3 and K_1.

$$\frac{C_{Bo} S_t}{k_o} = \frac{1}{K_1 k_3} + \frac{C_{Bo}}{k_3} \quad (16)$$

EXPERIMENTAL

1. Chemicals

All chemicals were of reagent grade and were used without fur-

Table 1. Experimental data of absorption rate in the CO_2/PGE and CO_2/GMA system

Solvent	C_{Bo} (kmol/m^3)	T (K)	r_{soap} (PGE) (cm^3/s)	r_{soap} (GMA) (cm^3/s)	T (K)	r_{soap} (PGE) (cm^3/s)	r_{soap} (GMA) (cm^3/s)
DMA	0	333	0.4587	0.4587	353	0.4184	0.4184
	0.1		0.5051	0.5181		0.4975	0.5236
	0.5		0.6623	0.7143		0.7353	0.8130
	1.0		0.8197	0.9009		0.9346	1.0101
	2.0		1.0471	1.1494		1.1765	1.2821
	0	343	0.4717	0.4717	363	0.3610	0.3610
	0.1		0.5405	0.5556		0.4545	0.4902
	0.5		0.7576	0.8130		0.7194	0.8065
	1.0		0.9524	1.0309		0.9174	1.0204
	2.0		1.2048	1.2987		1.1364	1.2346
NMP	0	333	0.3268	0.3268	353	0.4016	0.4016
	0.1		0.3953	0.4082		0.5650	0.5952
	0.5		0.6135	0.6623		1.0000	1.0870
	1.0		0.8065	0.8850		1.3333	1.4493
	2.0		1.0753	1.1905		1.7241	1.9231
	0	343	0.3690	0.3690	363	0.4464	0.4464
	0.1		0.4739	0.4950		0.6897	0.7353
	0.5		0.7813	0.8696		1.2987	1.4085
	1.0		1.0417	1.1628		1.7241	1.8868
	2.0		1.3699	1.5385		2.1739	2.4390
DMSO	0	343	0.2841	0.2841	353	0.4237	0.4237
	0.1		0.3353	0.3425		0.5464	0.5650
	0.5		0.5018	0.5263		0.9025	0.9709
	1.0		0.6540	0.6993		1.1905	1.2903
	2.0		0.8643	0.9346		1.5361	1.6863
	0	353	0.3413	0.3413	363	0.5128	0.5128
	0.1		0.4132	0.4310		0.7210	0.7246
	0.5		0.6390	0.7092		1.2642	1.3158
	1.0		0.8375	0.9259		1.6639	1.7544
	2.0		1.1013	1.2500		2.1008	2.2222

ther purification. Purity of both CO_2 and N_2 was greater than 99.9%. GMA, PGE, imidazole, beomoethane, tetraorthosilicate, 3-chloropropyltriethoxysilane, cetyltrimethylammonium bromide, tetramethylammounium chloride, and solvents such as *N*, *N*-dimethylacetamide (DMA), *N*-methyl-2-pyrrolidinone (NMP), and dimethyl sulfoxide (DMSO) were supplied by Aldrich Chemical Company, U.S.A.

2. Absorption Rate of CO_2

Absorption experiments were carried out in an agitated vessel and the experimental procedure was duplicated in detail as previously reported [24]. The absorption vessel was constructed of glass with an inside diameter of 0.073 m and a height of 0.151 m. Four equally spaced vertical baffles, each one-tenth of the vessel diameter in width, were attached to the internal wall of the vessel. The gas and liquid phase were agitated with an agitator driven by a 1/4 Hp variable speed motor. A straight impeller 0.034 m in length and 0.05 m in width was used as the liquid phase agitator and located at the middle position of the liquid phase. The surface area of the liquid was calculated as the ratio of the volume (300 cm^3) of added water to the measured height (7.3 cm) of water in the absorber, and was found to be 41.096 cm^2. The gas and liquid in the vessel were agitated at 50 rpm, which was adequate to maintain a planar gas-liquid interface. The value of the cumulative volume of the bubbles was measured by a soap bubbler with change in absorption time to obtain the absorption rate of CO_2. Each experiment was duplicated at least once under identical conditions. The volumetric rising rate (r_{soap}) of the bubble in the soap bubbler attached to the absorption vessel was assumed to be equal to the absorption rate of CO_2. The absorption experiments were carried out in a range of 0-2.0 kmol/m^3 of oxirane and 333-363 K at atmospheric pressure using pure CO_2, 2 g of catalyst, and solvents such as DMA, NMP and DMSO. The values of r_{soap} are listed in Table 1.

3. Synthesis of ID-CP-MS41

CP-MS41 was synthesized by hydrolysis of tetraorthosilicate, as the silicon source, with 3-chloropropyltriethoxysilane as an organosilane using cetyltrimethylammonium bromide as a template. ID-CP-MS41 was synthesized by immobilization of imidazole on mesoporous CP-MS41. The synthesis of MCM41 and CP-MS41 followed previous work reports [23]. The surface area and size of MCM41 were measured by BET isotherm and SEM, and were measured as 884.6 m^2/g and 5.0 mm, respectively.

4. Physical Properties

The viscosities (μ) of the solvent and oxirane solution were meas-

Table 2. Physical properties of the CO_2(A)/PGE and CO_2(A)/GMA system

T (K)	Solvent	C_{Ai} (kmol/m^3)	μ (cp)	$D_{Ao}\times10^9$ (m^2/s)	$D_{PGEo}\times10^9$ (m^2/s)	$D_{GMAo}\times10^9$ (m^2/s)	$k_{Lo}\times10^5$ (m/s)
333	DMA	0.0562	0.594	3.921	1.403	3.921	3.990
	NMP	0.0593	0.854	3.283	1.175	1.264	2.697
	DMSO	0.0528	1.082	2.489	0.890	0.959	2.633
343	DMA	0.0494	0.521	4.407	1.577	1.697	4.597
	NMP	0.0587	0.691	3.895	1.393	1.500	3.026
	DMSO	0.0524	0.761	3.242	1.160	1.248	3.136
353	DMA	0.0387	0.468	4.872	1.743	1.876	5.122
	NMP	0.0582	0.603	4.389	1.570	1.690	3.269
	DMSO	0.0520	0.498	4.426	1.583	1.704	3.860
363	DMA	0.0315	0.445	5.181	1.854	1.854	5.344
	NMP	0.0578	0.508	5.060	1.810	1.949	3.601
	DMSO	0.0517	0.345	5.813	2.080	2.080	4.625

ured using a Brookfield viscometer (Brookfield Eng. Lab. Inc, USA).

The solubility (C_{Ai}) of CO_2 was measured by the pressure measuring method, which involved measuring the pressure difference of CO_2 before and after equilibrium in the gas and liquid phases, similarly to a previously reported procedure [25], and the experimental procedure was duplicated in detail as previously reported [18].

The diffusivity (D_i) of CO_2 and oxiranes in the solvent and solution was estimated by the method modified with viscosity in the Stoke-Einstein equation [26] as follows:

$$D_i = 7.4\times10^{-12}\frac{TM_S^{1/2}}{\mu^{2/3}V_i} \tag{17}$$

The experimental data [27] were better correlated through the use of two-thirds power of the viscosity in Eq. (17) rather than a power of 1, as shown in the Stoke-Einstein equation.

The mass transfer coefficients (k_{Lo}) of CO_2 in various solvents were obtained from the measured r_{soup}. The mass transfer coefficient (k_L) in oxirane solution cannot be measured in the reaction of CO_2 with oxirane. In this study, k_L was estimated using the relationship [28] between k_{Lo} and the ratio of diffusivity in solution to that in solvent as follows:

$$k_L = k_{Lo}(D_A/D_{Ao})^{2/3} \tag{18}$$

These physical properties are listed in Table 2, and used to solve the simultaneous differential equations of Eq. (3) and (4).

RESULTS AND DISCUSSION

The experimental enhancement factor (β_{exp}) of CO_2 was obtained as the ratio of r_{soap} with reaction between CO_2 and oxirane to that without reaction. Fig. 1 shows typical plots of β_{exp} against C_{Bo} in DMA solution at various absorption temperatures for PGE and GMA, and demonstrates that β_{exp} increases with increasing C_{Bo} and temperature. These results are similar for other solvents. The solid line

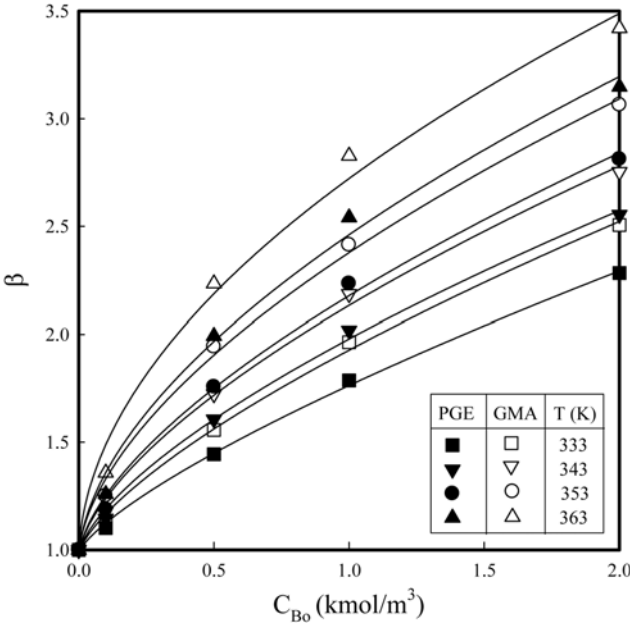

Fig. 1. β vs. C_{Bo} in DMA solution for PGA and GMA.

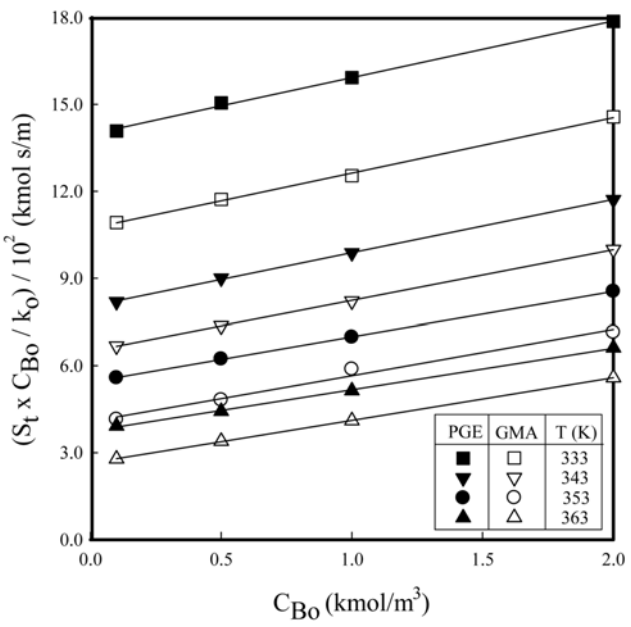

Fig. 2. S_tC_{Bo}/k_o vs. C_{Bo} in DMA solution for PGE and GMA.

presents the calculated value (β_{cal}) of β, to be discussed later. β_{exp} of GMA were a little larger than those of PGE.

The measured β_{exp} and Eq. (15) give k_o, and then, K_1 and k_3 are evaluated from the slope and intercept of the plots of $C_{Bo}S_t/k_o$ against C_{Bo} according to Eq. (16). Typical plots of S_tC_{Bo}/k_o against C_{Bo} are presented in Fig. 2 for the same conditions as shown in Fig. 1. The linear plots allow k_3 and K_1 to be obtained from the slope and intercept of the straight line according to Eq. (16), respectively. These results are similar for other solvents. The values of k_3 and K_1 for various solvents and temperatures are listed in Table 3. From the results of little difference of β_{exp} in Fig. 1, and k_3 and K_1 in Table 3, it seems that the intermediate complex of PGE and that of GMA in reaction (ii) have similar characteristics of electron formation to react with CO_2.

Table 3. Reaction rate constants of the reaction between CO_2 and oxirane

Oxirane	Temp. (K)	Solvent	$k_3\times10^3$ (1/m^2·s)	K_1 (m^3/kmol)
PGE	333	DMA	5.104	0.140
		NMP	6.041	0.137
		DMSO	7.097	0.126
	343	DMA	5.433	0.229
		NMP	6.518	0.187
		DMSO	7.506	0.153
	353	DMA	6.430	0.286
		NMP	7.043	0.264
		DMSO	8.127	0.221
	363	DMA	7.011	0.381
		NMP	7.668	0.356
		DMSO	8.730	0.325
GMA	333	DMA	5.236	0.178
		NMP	8.281	0.120
		DMSO	9.632	0.105
	343	DMA	5.735	0.268
		NMP	8.890	0.169
		DMSO	10.29	0.140
	353	DMA	6.292	0.390
		NMP	9.492	0.231
		DMSO	10.77	0.193
	363	DMA	6.801	0.556
		NMP	10.47	0.307
		DMSO	11.39	0.259

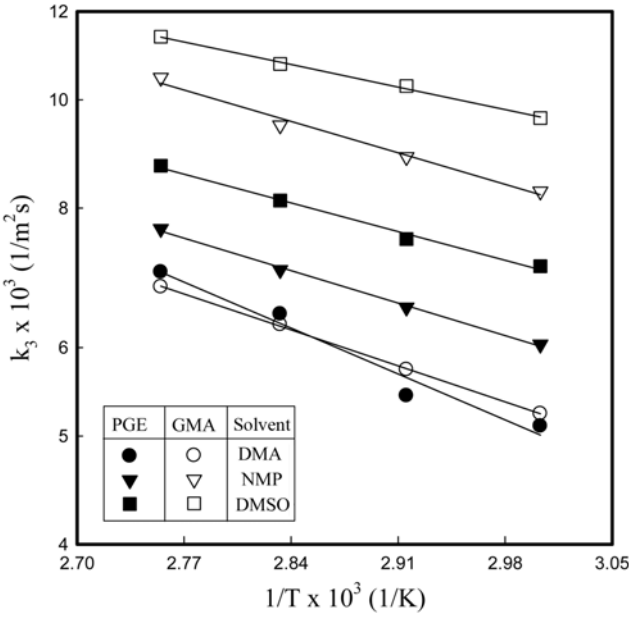

Fig. 3. Arrhenius plot of k_3 for PGE and GMA.

Fig. 3 shows the Arrhenius plots of k_3 with parameters of solvents and oxirane. The Arrhenius plots are linear and linear regression analysis of the Arrhenius plots with $r^2>0.960$ gives the activation energy for the forward reaction rate constant in the irreversible reaction of (iii), with 11.2, 8.0, and 7.0 kJ/mol for PGE and 8.8, 7.7, 5.5 kJ/mol for GMA in solvents of DMA, NMP, and DMSO, respectively.

Various empirical measurements of solvent effects have been proposed and correlated with the reaction rate constant [29]. Some measurements have a linear relationship to the solubility parameter (δ) of the solvent with logarithms of k_3 and K_1 plotted against δ [30] of DMA, NMP, and DMSO (18.2, 23.1, 24.6 (J/m^3)$^{0.5}$), respectively, in Fig. 4 and Fig. 5 for PGE and GMA, respectively.

The plots are linear, and k_3 and K_1 increase and decrease with higher δ, respectively. The solvent polarity increased with higher δ. Presumably, the increased instability and solvation of complex (C_1), arising from increased solvent polarity, enhance the dissociation reaction of C_1 and the reaction between C_1 and CO_2, as in an SN_1 (nucleophilic substitution) reaction [31]. The results in these figures suggest that the magnitude of the rate constants may be a function of the stabilization of the zwitterionic intermediates by the solvent [4]. The linear dependence of rate constant on δ, as shown in these figures, could be used to predict the rate constant in any organic solvent with δ.

Using the obtained values of k_3 and K_1 at given C_{Bo}, C_{Ai}, D_A, D_B, and k_L, The simultaneous differential equations of Eq. (8) and (9)

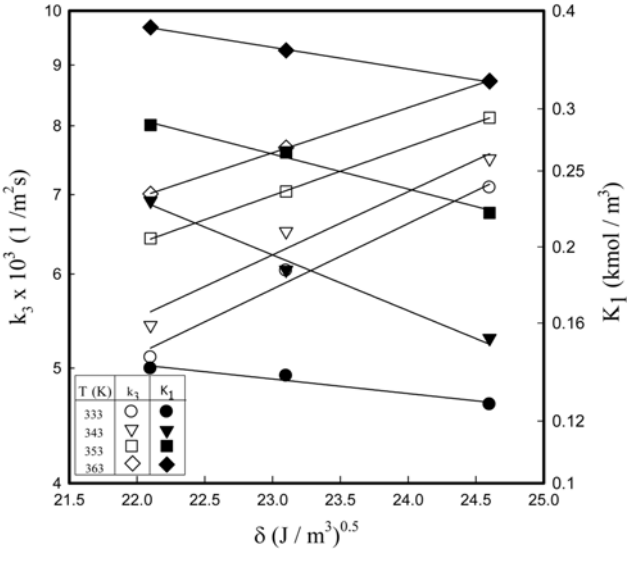

Fig. 4. Relationship between reaction rate constant and various solvent solubilities for PGE.

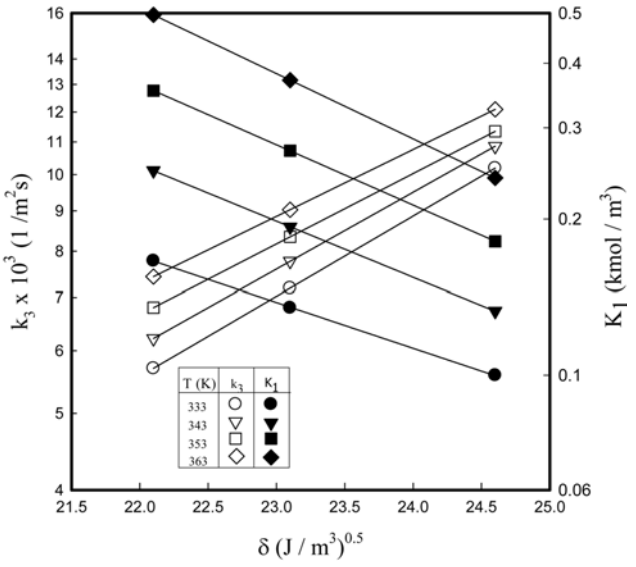

Fig. 5. Relationship between reaction rate constant and various solvent solubilities for GMA.

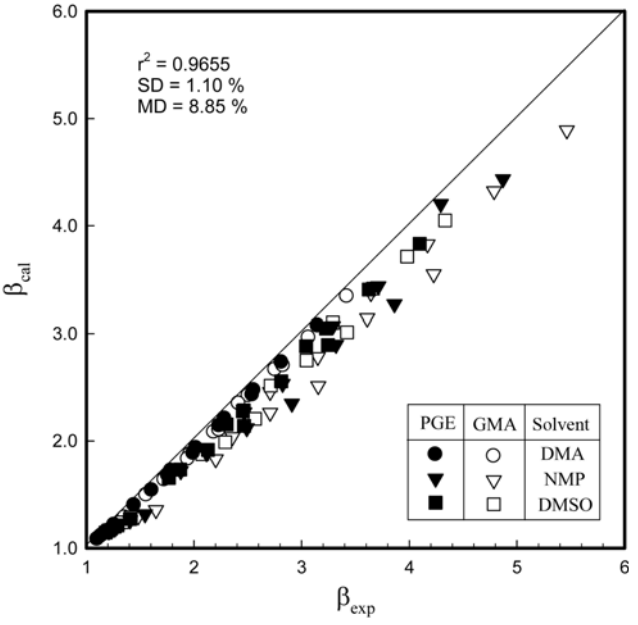

Fig. 6. Comparison of the calculated and measured values of the enhancement factor of CO_2 for PGE and GMA.

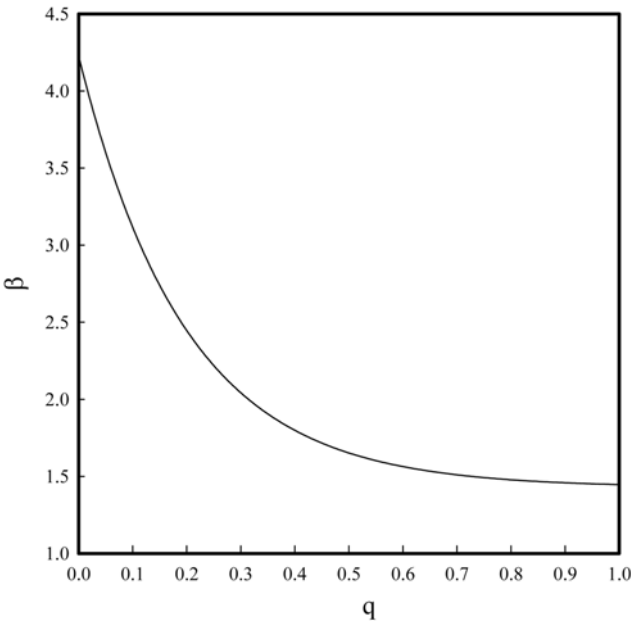

Fig. 7. Effect of q on β for M=20, a=0.1, a_L=0.0001, and r_{AB}=2.6.

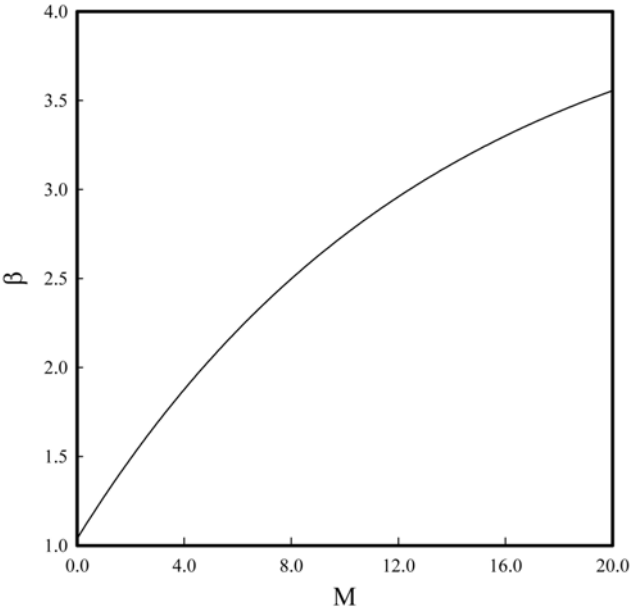

Fig. 8. Effect of M on β for q=0.05, a_L=0.0001, α=0.1, and r_{AB}=2.6.

with boundary conditions of Eq. (10) and (11) were numerically solved by a finite element method to give the profiles of C_A and C_B, and then, the β_{cal} was calculated from Eq. (12). Typical values are shown as symbols of the solid line in Fig. 1 and β_{exp} approaches to β_{cal}. All values of β_{exp} and β_{cal} for various solvents, oxirane concentrations and temperatures were compared in Fig. 6. β_{exp} approached β_{cal} within a mean deviation of 1.23% with r^2 of 0.96.

To observe the effect of physicochemical properties on β, β was obtained for various dimensionless variable of physicochemical properties such as q, M, α and a_L through the solution of the simultaneous differential equations of Eq. (8) and (9).

β, calculated from Eq. (12), were plotted for various q under the typical conditions of M of 20, α of 0.1, a_L of 0.0001, and r_{AB} of 2.6 in Fig. 7. β decreased with increasing q. This means that β decrease with increasing the physical absorption rate due to increase of C_{Ai} or decreasing the chemical absorption rate due to decrease of C_{Bo} by increase of q.

β, calculated from Eq. (12), were plotted for various M under the typical conditions of q of 0.05, α of 0.1, a_L of 0.0001, and r_{AB} of 2.6 in Fig. 8. β increased with increasing M, which means that β increase with increasing the chemical absorption rate due to increase of k_3, C_{Bo} and S_i, or decreasing the physical absorption rate due to decrease of k_L by increase of M.

β, calculated from Eq. (12), were plotted for various a under the

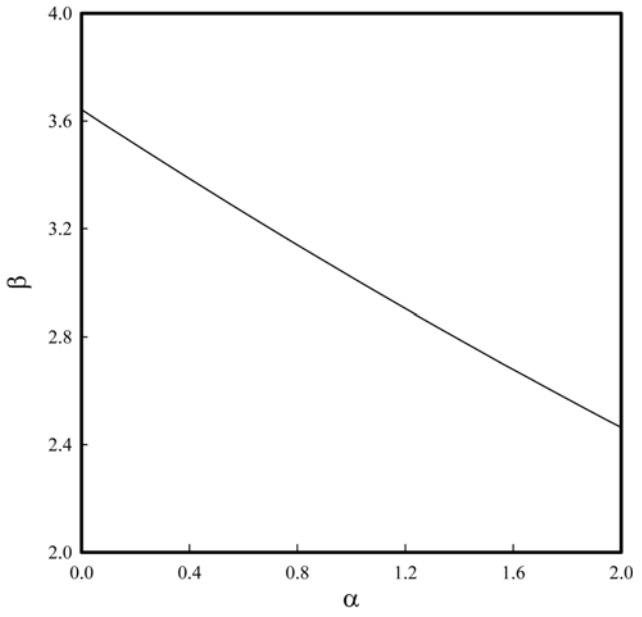

Fig. 9. Effect of α on β for M=20, q=0.05, a_L=0.0001, and r_{AB}=2.6.

typical conditions of q of 0.05, M of 20, a_L of 0.0001, and r_{AB} of 2.6 in Fig. 9. β decreased with increasing α. β should increase by increase of K_1 or C_{Bo} due to increase of α, as shown in Eq. (ii). From the definition of M, the other quantities, $k_3D_AS_t/k_L^2$, except α in M decrease with increasing α at the given value of M. Therefore, increase of the chemical absorption rate due to decrease of k_3, C_{Bo} and S_t, or increase of the physical absorption rate due to increase of k_L make β decreased as shown in Fig. 9.

β, calculated from Eq. (12), were plotted for various α under the typical conditions of q of 0.05, M of 20, a_L of 0.0001, and r_{AB} of 2.6 in Fig. 10. β was almost constant with increasing a_L from which it could be concluded that the effect of a_L on β is little.

β, calculated from Eq. (12), were plotted for various r_{AB} under the

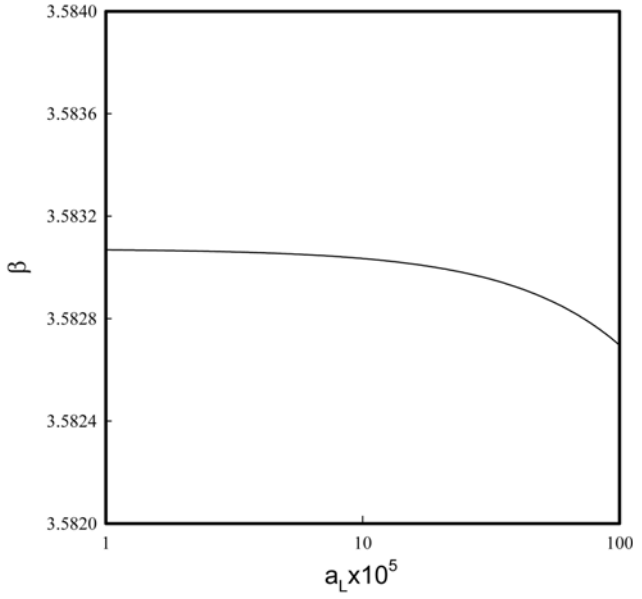

Fig. 10. Effect of a_L on β for M=20, q=0.05, α=0.1, and r_{AB}=2.6.

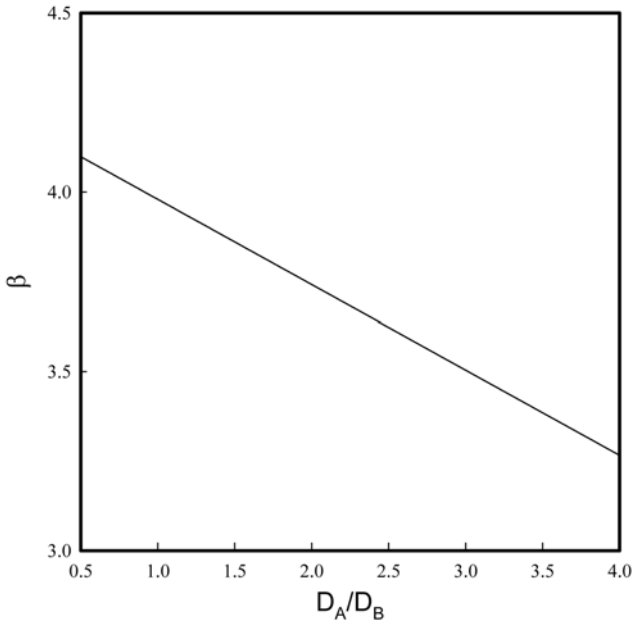

Fig. 11. Effect of r_{AB} on β for M=20, q=0.05, α=0.1, and a_L=0.0001.

typical conditions of q of 0.05, M of 20, α of 0.1, and a_L of 0.0001 in Fig. 11. β decreased with increasing r_{AB}. This means that β decrease due to decrease of mobility of oxirane by increase of the ratio of D_A to D_B.

CONCLUSIONS

Carbon dioxide was absorbed to react with oxiranes in solvent of DMA, NMP, and DMSO. A mathematical model for the CO_2 absorption associated with reaction with the oxirane was developed on the basis of the film theory with a non-linear reaction rate equation according to the zwitterion mechanism. Absorption data of CO_2 were used to obtain pseudo-first-order reaction rate constants, from which the elementary reaction rate constants were evaluated. The logarithmic reaction constants showed close to linear dependence on the solubility parameter of the solvent. The solution of dimensionless simultaneous differential equation for CO_2 and oxirane could predict the enhancement factor of CO_2 using the experimental variables. The reactivity of PGE with CO_2 is similar to that of GMA from the comparison of k_3 and K_1.

ACKNOWLEDGEMENTS

This work was supported by a grant (2006CCD11P011A-21-3-010) from the Energy Technology R&D of the Korea Energy Management Corporation and Korea Ministry of Environment (MOE) as Human resource development Project for Waste to Energy.

NOMENCLATURE

a_v : ratio of interfacial area of liquid to liquid volume [1/m]
C_i : concentration of species i [kmol/m^3]
D_i : diffusivity of species i [m^2/s]
H_a : Hatta number defined as $\sqrt{k_o D_A}/k_L$

k_o : pseudo-first-order reaction rate constant [1/s]
K_1 : reaction equilibrium constant defined as k_1/k_2 [m^3/kmol]
k_1 : forward reaction rate constant in reaction (ii) [$1/m^2 \cdot s$]
k_2 : backward reaction rate constant in reaction (ii) [kmol/$m^3 \cdot m^2 \cdot s$]
k_3 : forward reaction rate constant in reaction (iii) [$1/m^2 \cdot s$]
k_L : liquid-side mass transfer coefficient of CO_2 with reaction [m/s]
k_{Lo} : liquid-side mass transfer coefficient of CO_2 in solvent [m/s]
M_S : molecular weight of solvent [g/gmole]
r^2 : correlation coefficient
r_A : reaction rate of CO_2 [kmol/$m^3 \cdot s$]
r_{soup} : volumetric rising rate of the soup bubble [cm^3/s]
S_t : surface area of catalyst [m^2]
t : absorption time [s]
T : absorption temperature [K]
z : distance [m]
z_L : film thickness [m]

Greek Letters

β : enhancement factor of CO_2
δ : solubility parameter of solvent $(J/m^3)^{1/2}$
μ : viscosity of liquid [cP]

Subscripts

A : CO_2
B : PGE or GMA
cal : calculated value
exp : measured value
i : gas-liquid interface or species i
o : feed or solvent

REFERENCES

1. M. Aresta, *Carbon dioxide recovery and utilization*, Kluwer Academic Publishers, London (2003).
2. K. Weissermel and H. Arpe, *Industrial organic chemistry*, Wiley-VCH, Weinheim, New York (1997).
3. W. J. Peppel, *Ind. Eng. Chem*., **50**, 767 (1950).
4. G. Rokicki, *Makromol.Chem*., **186**, 331 (1985).
5. T. Aida and S. Inoue, *J. Am. Chem. Soc*., **105**, 1304 (1983).
6. Y. Nishikubo, T. Kato, S. Sugimoto, M. Tomoi and S. Ishigaki, *Macromolecules*, **23**, 3406 (1990).
7. N. Kihara and T. Endo, *Macromolecules*, **25**, 4824 (1992).
8. T. Nishikubo, A. Kameyama, J. Yamashida, M. Tomoi and W. Fukuda, *J. Polym. Sci.*, *Part A, Polym. Chem*., **31**, 939 (1993).
9. T. Nishikubo, A. Kameyama, J. Yamashida, T. Hukumitsu, C. Maejima and M. Tomoi, *J. Polym. Sci., Part A, Polym. Chem*., **33**, 1011 (1995).
10. C. M. Starks, C. L. Liotta and M. Halpern, *Phase transfer catalysis*, Chapman & Hall, New York (1994).
11. L. K. Daraiswany and M. M. Sharma, *Heterogeneous reaction: Analysis, example and reactor design*, John Wiley & Sons, New York (1980).
12. S. W. Park, D. W. Park, T. Y. Kim, M. Y. Park and K. J. Oh, *Catal. Today*, **98**, 493 (2004).
13. S. W. Park, D. W. Park and J. W. Lee, *Korean J. Chem. Eng*., **23**, 645 (2006).
14. S. W. Park, B. S. Choi, B. D. Lee, D. W. Park and S. S. Kim, *Sep. Sci., Technol*., **41**, 829 (2006).
15. Y. S. Son, S. W. Park, D. W. Park, K. J. Oh and S. S. Kim, *Korean J. Chem. Eng.*, **26**, 1359 (2009).
16. S. W. Park, B. S. Choi, D. W. Park, S. S. Kim and J. W. Lee, *Korean J. Chem. Eng.*, **24**, 953 (2007).
17. S. W. Park, B. S. Choi, D. W. Park, K. J. Oh and J. W. Lee, *Green Chem*., **9**, 605 (2007).
18. Y. S. Son, S. W. Park, D. W. Park, K. J. Oh and S. S. Kim, *Korean J. Chem. Eng*., **26**, 783 (2009).
19. C. T. Kresge, M. E. Leonowicz, W. J. Roth, J. C. Vartuli and J. S. Beck, *Nature*, **359**, 710 (1992).
20. J. S. Beck, J. C. Vartuli, W. J. Roth, M. E. Leonowicz, C. T. Kresge, K. D. Schmitt, C. T. W. Chu, D. H. Olson, E. W. Sheppard, S. B. McCullen, J. B. Higgins and J. L. Schlenker, *J. Am. Chem. Soc*., **114**, 10834 (1992).
21. A. Bhaumik and T. Tatsumi, *J. Catal*., **189**, 31 (2000).
22. S. Xu, C. Huang, J. Zhang, J. Liu and B. Chen, *Korean J. Chem. Eng*., **26**, 985 (2009).
23. S. Udayakumar, S. W. Park, D. W. Park and B. S. Choi, *Catal. Commun*., **9**, 1563 (2008).
24. S. W. Park, D. W. Park, K. J. Oh and S. S. Kim, *Sep. Sci., Technol*., **41**, 543 (2009).
25. M. L Kennard and A. Meisen, *J. Chem. Eng. Data*, **29**, 309 (1984).
26. R. C. Reid, J. M. Prausnitz and T. K. Sherwwod, *The properties of gases and liquids*, McGraw-Hill, New York (1977).
27. E. L. Cussler, *Diffusion*, Cambridge University Press, New York (1984).
28. G. Carta and R. L. Pigford, *Ind. Eng. Chem. Fundam*., **22**, 329 (1983).
29. H. F. Herbrandson and F. B. Neufeld, *J. Org. Chem*., **31**, 1140 (1966).
30. J. Brandrup and E. H. Immergut, *Polymer Handbook*, Second Ed., John Wiley & Sons, New York (1975).
31. R. T. Morrison and R. N. Boyd, *Organic Chemistry*, Fourth Ed., Allyn and Bacon, Inc., Toronto (1983).